AD-A166 931 DESIGN AND STUDY OF NEW ORGANIC POLYMER CRYSTALS AND THIN FILMS(U) PENNSYLVANIA UNIV PHILADELPHIA DEPT OF PHYSICS A F GARITO 31 DEC 83 DAAK70-77-C-0045 1/1

UNCLASSIFIED F/G 20/2 NL

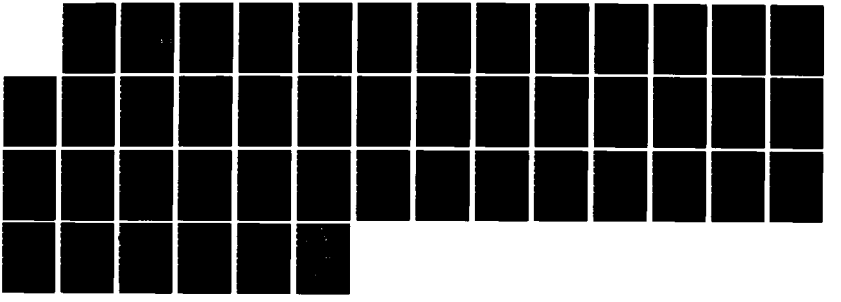

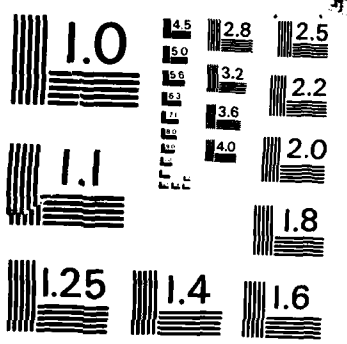

DESIGN AND STUDY OF NEW ORGANIC POLYMER CRYSTALS AND THIN FILMS

Defense Advanced Research Projects Agency/MATS

Order Number DAAK70-77-C-0045/DAAK70-83-C-0074

Monitored by Army Night Vision and Electrooptics Laboratory

Principal Investigator: Position:

Prof. A.F. Garito — Professor of Physics
(215)898-5810

School: Department: Physics

Faculty of Arts and Sciences

Starting Date: Expiration Date:

October 1, 1976 — December 31, 1983

Reporting Period: October 1, 1976 - December 31, 1983

Corporate Name of University:

The Trustees of the University of Pennsylvania
(a Pennsylvania Non-Profit Corporation)

Contracting Office:

Office of Research Administration
3451 Walnut Street
Philadelphia, PA 19104

Technical Report

Nonlinear Optical Properties of Organic and Polymer Crystals and Films

A.F. Garito, C.C Teng, K.Y. Wong and O. Zammanai'Khamiri

Department of Physics

University of Pennsylvania

Philadelphia, PA 19104-3859

Spring 1984

The work reported in this document was performed at the University of Pennsylvania, Department of Physics. This work was sponsored by the Defence Advanced Research Projects Agency under Contract DAAK-700-77-C-0045. This report may be reproduced to satisfy needs of U.S. Government agencies.

The views and conclusions contained in this document are those of the contractor and should not be interpreted as necessarily representing the official policies, either expressed or implied, of the United States Government.

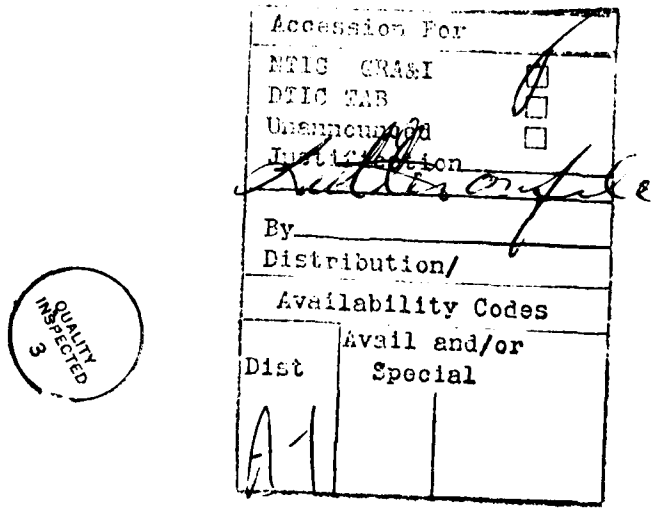

ABSTRACT

Physical studies of nonlinear optical properties of organic and polymer structures have demonstrated exceptionally large second and third order nonlinear optical responses that are important to the fields of nonlinear optics and optical device technologies. These unusual responses have been exhibited by a large number of structures, phases, and states that include organic solids and films, single crystal polymers, Langmuir-Blodgett films, liquid crystals, and liquid crystal polymers. Experimental and theoretical studies of such systems have achieved significant advances in the understanding of these exceptional macroscopic nonlinear optical responses based on theoretically calculated microscopic electronic mechanisms, especially the role of electron-electron correlations and highly charge correlated electron excited states. Combined theory and experiment has led to the recent discovery of liquid crystal polymerization of divinyldiacetylene monomers to form highly conjugated liquid crystal polymers exhibiting large second and third order nonlinear optical responses.

This report has served as a major review article in the field of nonlinear optics and was published in Molecular Crystals and Liquid Crystals as part of an international symposium proceedings.

I. INTRODUCTION

This article concerns the macroscopic nonlinear optical responses of organic and polymeric structures and the fundamental understanding of the relations and origins of nonlinear processes to the nature of electronic excitations and their interactions. As natural developments in studies of nonlinear optical phenomena, the recent demonstrations of phase conjugated wave generation[1], optical bistable states,[2] and exceptionally large nonlinear optical susceptibilities in organic and polymeric materials[3,4] have stimulated considerable growth in research and development activities in centers throughout the world. These intriguing phenomena suggest a wide variety of potential applications in future optical telecommunications, image reconstruction, integrated optics, optical signal switching and processing, data storage, and optical memory and logic technologies. We believe the recent advances in nonlinear optics research can be rapidly accelerated and enlarged through fundamental studies of organic and polymer crystals and films.

In recent years, theoretical and experimental interest has centered on the origin of the exceptional second[5] and third order[6] nonlinear optical responses observed for certain organic and polymeric structures, particularly as exhibited by the second order processes of second harmonic generation (SHG) and linear electro-optic effect (LEO) properties. The case of 2-methyl-4-nitroaniline (MNA) (Figure 1) serves as an important example[7-9]. MNA crystals possess SHG and LEO figures of merit 50 times those of common dielectric insulators such as potassium dihydrogenphosphate (KDP) and 200 times those of semiconductors such as gallium arsenide (GaAs)[3]. The origin of such unusual nonlinear optical responses resides in the π-electron structure (Figure 2), and the current view is that the π-electron molecular structure represents the finite chain limit to the infinite conjugated polymer chain.

II. NONLINEAR OPTICAL PROPERTIES AND ORGANIC NONLINEAR MEDIA

Nonlinear optical responses are expressed through the constitutive relation for the dielectric polarization P(t) of a nonlinear medium in an intense optical field $E(t) = Re(Ee^{i\omega t})$[10]

$$P(t) = \chi^{(1)}E(t) + \chi^{(2)}E^2(t) + \chi^{(3)}E^3(t) + \ldots \quad (1)$$

The first and third order terms in odd powers of E(t) are common for all materials. $\chi^{(1)}$ represents linear optics, and $\chi^{(3)}$ third order nonlinear processes. Important examples include third harmonic generation ($\omega + \omega + \omega = 3\omega$) and self-focusing ($\omega - \omega + \omega = \omega$). The second order response $\chi^{(2)}$ occurs only in noncentrosymmetric media; that is, those lacking a natural center of inversion symmetry. In general for second order processes, fundamental frequencies at ω_1 and ω_2 combine to create a third frequency at ω_3 ($\omega_1 \pm \omega_2 = \omega_3$). For example, having ω_1 and ω_2 the same, the sum leads to second harmonic generation (SHG) ($\omega + \omega = 2\omega$), and the difference, optical rectification ($\omega - \omega = 0$). Moving one frequency down to dc results in the linear electrooptic effect (LEO) ($\omega + 0 = \omega$). Thus, there are a large number of important nonlinear optical processes over the entire

frequency range, and the frequency dependences or dispersions, of $\chi^{(2)}$ and $\chi^{(3)}$ are fundamentally important properties of the nonlinear medium.

There are numerous ways to induce a nonlinear optical polarization in a medium. They generally involve either absorptive, or reactive, nonlinear responses. In an absorptive response, the absorbed photon causes an actual transformation in the physical state of the nonlinear medium. There is a net population change in the statistical average of the excited centers, and the response is accompanied by real optical loss of the propagating waves. Examples include photorefractive migration of charge, resonant saturable absorption, and high order field alignment in liquid crystals.

In contrast, a reactive nonlinear response is due to lossless virtual optical excitations in the nonlinear medium that do not involve net population changes or any material transformations. Examples include non-resonant harmonic generation, frequency mixing, and optical Kerr effects. By far the shortest response times occur in reactive nonlinear media since reactive responses do not involve relatively slow material changes of the nonlinear medium. Moreover, among the possible virtual excitations of reactive responses, electron excitations of order 10^{-15} seconds are intrinsically faster than phonon excitations which involve much slower nuclear displacements and vibrations of order 10^{-12} seconds.

For large classes of conjugated molecules and polymer structures, the remarkable property is that the nonlinear optical responses are dominated by lossless virtual excitations of the π-electron states, especially those possessing large charge correlations. This property is most readily observable in second order responses. For example, in crystalline solids, only electronic excitations contribute to second harmonic generation, whereas both electron and phonon

excitations contribute to the linear electro-optic effect. For MNA (Figure 1), for example, the large second harmonic susceptibility $\chi^{(2)}_{111}(-2\omega;\omega,\omega)$ of $500 \pm 125 \times 10^{-12}$ m/V was shown to be the same as the linear electrooptic susceptibility $\chi^{(2)}_{111}(-\omega;\omega,0) = 500 \pm 150 \times 10^{-12}$ m/V within experimental error, demonstrating that the second order response is primarily purely electronic with little or no lattice contribution, and thus intrinsically fast[8]. Examples at the molecular level include the frequency dependence of the microscopic second order response of organic molecular structures, such as MNA, that is described below[11,12].

III. ORIGIN OF $\chi^{(2)}$ AND HIGHLY CHARGE CORRELATED π-ELECTRON STATES

Currently, the π-electron excitations are viewed as occurring on individual molecular, or polymer, sites and providing macroscopic sources of nonlinear response through the corresponding on-site microscopic nonlinear optical susceptibility. Since intramolecular bonding interactions (100 kcal/mole) are much stronger than relatively weak van der Waals intermolecular interactions (1 kcal/mole), each molecular, or polymer, unit is essentially an independent source of nonlinear response. Each term in the macroscopic polarization of eqn. (1) can thus be expressed as comprised of the corresponding microscopic nonlinear optical response

$$p(t) = \alpha E(t) + \beta E^2(t) + \gamma E^3(t) + \ldots \quad (2)$$

where α is the linear polarizability, and β and γ are the second and third order nonlinear electronic susceptibilities, respectively. In the rigid lattice gas approximation, the macroscopic $\chi^{(2)}$, for example, is expressed as

$$\chi^{(2)}_{ijk}(-\omega_3; \omega_1, \omega_2) =$$

$$Nf^{\omega_1} f^{\omega_2} f^{\omega_3} \langle \beta_{ijk}(-\omega_3; \omega_1, \omega_2) \rangle \qquad (3)$$

where N is the number of sites per unit volume, f^{ω_i} represent small local field corrections, and β_{ijk} is averaged over the unit cell. An analogous expression is obtained for the $\chi^{(3)}$ response. Thus, unlike inorganic semiconductors and dielectric insulators, the problem of understanding the origin of the large macroscopic $\chi^{(2)}$, or $\chi^{(3)}$, is reduced to experimental and theoretical studies of the corresponding microscopic β, or γ, of single molecular, or polymer, units, making up the optically nonlinear organic solid.

The quantum-field theory treatment[12] of $\beta_{ijk}(-2\omega;\omega,\omega)$ provides a convenient diagrammatic representation of the three-wave-mixing process as shown by the space-time diagrams in Figure 3. A ground state $|g\rangle$ molecule with eignestates $|n\rangle$ and $|n'\rangle$ and eigenvalues $\hbar\omega_{\mp}$ in an electromagnetic field $\vec{E}(t) = Re(\vec{E}^{\omega} e^{\mp i\omega t})$ responds to the perturbing Hamiltonian $H' = e\vec{E}^{\omega}(t)\cdot\vec{r}$ in the dipole approximation that induces an electronic polarization in the molecular structure,

$$P_1^{2\omega} = \sum_{j,k} \beta_{ijk}(-2\omega; \omega, \omega) E_f^{\omega} E_k^{\omega} \qquad (4)$$

where both the fundamental ω and created harmonic 2ω frequencies are below electronic resonances but well above vibrational and rotational modes.

The quantized field is given by the

expression

$$\vec{E}^{\omega}(t) = -\frac{1}{c}\frac{\partial \vec{A}}{\partial t} = -i\left[\frac{2\pi\hbar\omega}{V}\right]^{1/2} \sum_{\vec{k},\alpha} (a^{\dagger}_{k,\alpha}\hat{\epsilon}_{\alpha}e^{i\omega t} - a_{\vec{k},\alpha}\hat{\epsilon}_{\alpha}e^{-i\omega t}), \tag{5}$$

where $a^{+}(a)$ is the photon creation (annihilation) operator; $\hat{\epsilon}$, the polarization unit vector with $\alpha = 1,2$; k, the unit direction vector; and V, the normalization volume. The resulting quantum-field theory expression for β_{ijk} is

$$\begin{aligned}
&\beta_{ijk} + \beta_{ikj} = \\
&-\frac{e^3}{4\hbar^2}\Bigg[\sum_{\substack{n\neq n'\\ n'\neq g\\ n\neq g}} (r_{gn'}{}^{i}r_{n'n}{}^{j}r_{gn}{}^{k} + r_{gn'}{}^{k}r_{n'n}{}^{j}r_{gn}{}^{i})\left(\frac{1}{(\omega_{n'g}-\omega)(\omega_{ng}+\omega)} + \frac{1}{(\omega_{n'g}+\omega)(\omega_{ng}-\omega)}\right) \\
&\quad + (r_{gn'}{}^{i}r_{n'n}{}^{j}r_{gn}{}^{k} + r_{gn'}{}^{j}r_{n'n}{}^{k}r_{gn}{}^{i})\left(\frac{1}{(\omega_{n'g}+2\omega)(\omega_{ng}+\omega)} + \frac{1}{(\omega_{n'g}-2\omega)(\omega_{ng}-\omega)}\right) \\
&\quad + (r_{gn'}{}^{j}r_{n'n}{}^{k}r_{gn}{}^{i} + r_{gn'}{}^{k}r_{n'n}{}^{j}r_{gn}{}^{i})\left(\frac{1}{(\omega_{n'g}-\omega)(\omega_{ng}-2\omega)} + \frac{1}{(\omega_{n'g}+\omega)(\omega_{ng}+2\omega)}\right) \\
&\quad + 4\sum_{n}[r_{gn}{}^{j}r_{gn}{}^{k}\Delta r_{n}{}^{i}(\omega_{ng}{}^{2}-4\omega^{2}) + r_{gn}{}^{i}(r_{gn}{}^{k}\Delta r_{n}{}^{j} + r_{gn}{}^{j}\Delta r_{n}{}^{k})(\omega_{ng}{}^{2}+2\omega^{2})] \\
&\qquad\qquad \times\frac{1}{(\omega_{ng}{}^{2}-\omega^{2})(\omega_{ng}{}^{2}-4\omega^{2})}\Bigg]
\end{aligned} \tag{6}$$

where summations are over the complete sets of eigenstates $|n\rangle$ and $|n'\rangle$ of the unperturbed system. The quantities such as r^{i}_{gn} and r^{i}_{nn} are matrix elements of the i^{th} components of the dipole operator for the molecule between the unperturbed ground (g) and excited states (n and n') $r^{i}_{gn} = \langle g|r_i|n\rangle$, and between two excited states $r^{i}_{nn'} = \langle n|r_i|n'\rangle$, respectively; $\Delta r^{i}_{n} = r^{i}_{nn} - r^{i}_{gg}$ is the difference between the excited and ground state dipole moments; ω is the frequency of the applied optical field; and $\omega_{ng} = \omega_{n} - \omega_{g}$ is the difference between the excited and ground state frequencies.

The π-electron states $|n\rangle$ and $|n'\rangle$ are true many-body states because electron-electron correlations due to natural repulsive Coulomb interactions tend to localize the otherwise delocalized electrons. In calculating β and its dispersion from eqn. (6), these many-body states can be obtained by a self-consistent field procedure (SCF) including configuration interactions (CI) for electron-electron correlations (Figure 4)[5]. Detailed theoretical analyses of the contributions to β for several molecular structures have demonstrated that the nature of the electron-electron correlations determines the nonlinear response of the organic medium[13].

Of the many π-electron excited states in conjugated structures, only those states possessing highly asymmetric charge correlations are principally responsible for the measured magnitude, sign and dispersion of β. These states characteristically possess relatively large values for both the transition moment $\vec{\mu}_{ng}^{i} = -er_{g}^{i}$ and the dipole moment difference $\Delta\vec{\mu}_{n}^{i} = -er_{n}^{i}$ important in eqn. (6) for β[5]. For MNA, for example, of the nine lowest energy singlet excited states, only two highly charge correlated π-electron states uniquely determine β[14]. The electron wavefunction contour diagrams of the MNA ground state and one of the principal excited states are given in Figure 5 along with the corresponding values for $\vec{\mu}_{gn}^{x}$ and $\Delta\vec{\mu}_{n}^{x}$. Upon virtual excitation, the many-body excited state clearly exhibits redistribution of electron density from the region of the NH_2 donor group to the NO_2 acceptor group and its neighboring sites, giving the excited state a highly charge correlated feature along the dipolar x axis of the molecule. Similar results have been obtained for a wide range of molecular structures such as quinoids[15], stilbenes, polyenes, acetylenes, and diacetylenes[13]. The basic mechanism of charge correlations always appears to determine the nonlinear optical response.

IV. DISPERSION OF β FOR ORGANIC SYSTEMS

The microscopic susceptibility β and its dispersion is experimentally determined by electric field induced second harmonic generation (DCSHG) measurements of liquid solutions[12] as illustrated in Figure 6. An applied DC field E^{O} removes the natural center of inversion symmetry of the solution, and the second harmonic signal is measured using the wedge Maker fringe method. The measured polarization at the second harmonic frequency 2ω produced by applied fields at ω and zero is given by

$$P_1^{2\omega} = \Gamma_{1111} E_1^{0} E_1^{\omega} E_1^{\omega} \tag{7}$$

with statistical averaging over the Boltzmann distribution of molecules and all laboratory fields having a common linear polarization. The term $\Gamma_{1111}E_1^{\emptyset}$ is the effective second harmonic susceptibility of the liquid solution. When the ground state dipole moment $\vec{\mu}$ is aligned along the molecular x axis, Γ_{1111} is given by

$$\Gamma_{1111} \equiv \Gamma_L = N f^{0} (f^{\omega})^2 f^{2\omega} \left[\gamma + \frac{\beta_x \mu}{5 k_B T} \right], \tag{8}$$

where γ is the microscopic third order susceptibility, which is negligibly small for conjugated molecules $\gamma << \beta_x \mu / 5k_B T$; β_x is the vector part of β_{ijk},

$$\beta_x = \beta_{xxx} + 1/3(\beta_{xyy} + \beta_{xzz} + 2\beta_{yyx} + 2\beta_{zzx}) \tag{9}$$

However, local field effects and solution interactions can lead to widely differing values for β.[12] By combined experimental studies of DCSHG, dielectric constant, index of refraction, and specific volume, an infinite dilution extrapolation method for β was developed that accounts for local fields and minimizes solute-solute and solvent-solvent interactions[16]. Theoretical gas phase values of β can then be compared to infinite dilution values if solvent induced shifts of the singlet-singlet electronic excitations of the measured system are included[11].

From the DCSHG measurements of β, the frequency dependent experimental values β_x^{expt} (Figure 7) for MNA in dioxane are observed to increase smoothly as the fundamental frequency ω is increased and begin to diverge as 2ω approaches the excitation frequency ($\hbar\omega_{ng}$ ~ 3.5 eV), which corresponds to the first major optical excitation to the charge correlated excited states of MNA dissolved in dioxane. The β_x^{expt} values are red shifted to lower energies compared to the theoretical gas phase dispersion curve due to solvent induced (solvatochromic) shifts $\hbar\omega_{ng}$ to lower energies of the gas phase singlet-singlet excitation energies. These shifts are easily observable in spectra for MNA measured in the gas phase and in dilute dioxane solutions (Figure 8)[12].

It has long been known that solvent-induced shifts in $\pi - \pi^*$ excitation energies are principally caused by dipole mediated interactions that change the difference between the solute ground state and excited state dipole moments. The shifts in excitation energy $\hbar\omega_{ng}$ in the dipole approximation is given by[17]

$$\hbar\Delta\omega_{ng} = A\,\Delta\mu_{ng}(\mu_n + \mu_g) + B\,\Delta\mu_{ng}\,\mu_g \,. \qquad (10)$$

where

$$A \equiv \frac{1}{a^3}\frac{n^2-1}{2n^2+1},$$

$$B \equiv \frac{2}{a^3}\left[\frac{\epsilon-1}{2\epsilon+1} - \frac{n^2-1}{2n^2+1}\right],$$

with n the index of refraction of the solution; ϵ, the dielectric constant of the solution; a, the effective cavity radius of the molecular site; μ_n and μ_g the solute dipole moments for the excited and ground states, respectively. The first and second terms, respectively, are the reaction field experienced by the permanent dipole moment of the solute due to interaction with (1) the induced dipole moments of the surrounding molecules, and (2) the permanent dipole moments of the solvent and of other solute molecules at relatively high concentrations.

New values for the state energies $\hbar\omega_{ng}$ of the excited states for MNA in dioxane were obtained using eqn. (10) and the SCF-CI calculations for the frequency dependent β of MNA were repeated. The resulting theoretical dispersion curve for MNA is directly compared with the frequency dependent experimental values β_x^{expt} in Figure 7. Within experimental error, the agreement between experiment and theory is quite satisfactory. One can conclude, therefore, that the microscopic electronic mechanism whereby virtual excitations to highly charge correlated π-electron excited states result in exceptional second order nonlinear optical responses is essentially correct and that the theoretical SCF-CI calculation represents a suitable procedure for determining and analyzing the intrinsic β components. Moreover, in regard to experimental methodology, these results demonstrate that DCSHG liquid solutions deter-

minations of β must account for solvent induced changes in the electronic excitations of the measured system. For $\pi - \pi^*$ excitations, classical reaction field methods appear to adequately account for these solvent effects as dipole mediated interactions.

Finally, it is important to point out that there is a direct relationship between the electronic second order nonlinear optical response (eqn. (6)) and dipole mediated solvent shifts (eqn. (10)) of optical excitations, or solvatochromism. Important to the development of new optically nonlinear structures, one can initially identify by simple independent measurements of the solvent shift $\hbar\omega_{ng}$ suitable structures possessing optically nonlinear responses optimized for experimental studies, or optical device applications. These structures would include organics, charge-transfer salts, dyes, liquid crystals, polymers, and even organic transition-metal complexes[12].

V. SECOND ORDER NONLINEAR OPTICAL PROCESSES AND STRUCTURALLY ORDERED POYMERS: DISUBSTITUTED DIACETYELNE POLYMERS

The same highly charge correlated π-electron states can be systematically incorporated into macromolecular polymer structures by introducing optically nonlinear molecular units as either (i) pendant side groups, or (ii) monomer repeat units, of the polymer main chain. The important case of the second order nonlinear optical process of second harmonic generation will be discussed although many of the same features apply to third order processes. Along with the symmetry requirement of noncentrosymmetry, several basic conditions are required of the nonlinear polymeric medium for efficient second order processes. The nonlinear medium should exhibit (i) optical transparency over the frequency range of the fundamental and second

harmonic waves to avoid optical loss; (ii) phase matching where the optical birefringence cancels the natural dispersion in order to obtain equal indices of refraction at the fundamental and second harmonic frequencies for efficient second harmonic generation; and (iii) long range structural order so that the microscopic β components are not diminished, or cancelled entirely, over large regions of the nonlinear medium.

Phase matched second harmonic generation in single crystal polymers was first demonstrated in noncentrosymmetric diacetylene polymers substituted with MNA molecular sites as pendant side groups of the repeat units of the conjugated polymer main chain.[18] Diacetylene polymer structures were selected to satisfy the basic conditions for second order nonlinear optical processes but also to allow systematic development and understanding of the fundamental physics through combined theory and experiment.

Optically nonlinear single crystal diacetylene polymers are formed by polymerization of disubstituted diacetylene monomers in the solid state (Figure 9).[19] With R as the acentric, or even chiral, optically nonlinear side group, diacetylene monomers crystallize as linear arrays that can be initiated to polymerize by thermal annealing, by irradiation with uv, x-rays[20] or electron beams, and in some cases, even mechanically . The resulting diacetylene polymer chain possesses three dimensional long range order as illustrated, for example, by the unit cell polymer structure of DNP [1,6-bis(2,4-dinitrophenoxy)-2,4-hexadyne] (Figure 10) from our early work of incorporating optically nonlinear dinitrophenoxy units as pendant side groups[21].

In addition to the π-electron system contained in the R group substituents, the polymer conjugated chain possesses a π-electron band structure that, in general, exhibits optical transparency from approximately the mid-visible region into the near infrared, leading to in-

dices of refraction in the range 1.6 to 2. The natural structural anisotropy of the ordered polymer chains leads to large optical birefringence important to phase matching. Under polarized visible light, single crystals exhibit a lustrous metal-like reflectance for polarization along the chain axis direction and a rich blue, or green, reflectance for polarization perpendicular to the chain axis. Diacetylene polymer crystals also possess exceptional radiation and mechanical damage resistance; for instance, radiation damage thresholds have been observed as high as 1 gigawatt/cm^2 for 25 nanosecond pulses at 1.89 μm[3].

Theoretical SCF-CI calculations reveal that the highly charge correlated π -electron excited states of MNA molecular units are present in MNA substituted diacetylene monomers such as MNADA and NTDA (Figure 11)[13,18]. DCSHG measurements of the MNADA monomer, for example, show the same large value of β as MNA alone (Figure 11)[22]. In the solid state, the phase matched second harmonic signal increases as the diacetylene polymer is formed. Figure 12 shows early data of the second harmonic intensity for NTDA microcrystals polymerized under x-ray radiation. As the polymer forms, the second harmonic intensity steadily increases to 10-15 times the lithium iodate reference signal. The constant second harmonic intensity at high x-ray dosages beyond that required for complete polymer formation confirms that the observed signal is intrinsic and not due to x-ray induced defect formation[18].

In addition to MNA and DNP pendant groups, other molecular units intrinsically possessing larger microscopic susceptibilities can be substituted on diacetylene monomers (Figure 13). Development of the new quinoid containing structures is based on earlier theoretical studies[15]. An exceptionally large β value of -170 x 10^{-30} esu for DCNQA (7,7-diamino-8,8-dicyanoquinodimethane) resulting from charge correlations in the π -electron excited states was predicted and subsequently confirmed by DCSHG experiments on

the related derivative DCNQI [2-(4-dicyanomethylenecyclohexa-2,5-dienylidine)-imidazolidine] with β of $-240 \pm 60 \times 10^{-30}$ esu. These classes of structures continue under study particularly as optical guided wave structures fabricated by Langmuir-Blodgett methods[23].

VI LIQUID CRYSTAL POLYMERIZATION AND LIQUID CRYSTAL POLYMERS: DIVINYLDIACETYLENES

In the diacetylene monomers and polymers exhibiting phase matched second harmonic generation, such as MNADA, both theory and experiment suggest that the charge correlated states remain on the MNA side group because the connecting methylene carbon group essentially acts as a π-electron blocking group. Our SCF-CI calculations of the electronic structures of alternate diacetylene monomer structures show that removal of the methylene carbon group, or replacement by an ethylene group causes extensive delocalization of the π-electron states over the entire monomer structure. The simplest structures that illustrate the delocalization are centrosymmetric divinyldiacetylene structures (Figure 14).

The contour diagrams (Figure 15) of the principal ground state and low lying singlet (^1B_u) π-electron excited state for bis(p-methylphenyl)-divinyldiacetylene (DVDA1) summarizes a number of remarkable features[24]. Upon optical excitation, the π-electron distribution thoroughly reorganizes over every carbon site comprising the DVDA1 structure. There is no distinction between the aromatic ring and diacetylene states; entirely new DVDA π-electron states are formed. Second, charge correlations are present in the lowest lying ^1B_u excited state with the most pronounced charge correlations occuring on the first vinylic carbon atom adjacent to the phenyl ring structure. The associated optical transition moment $\vec{\mu}^x_{ng}$ for this state is greater than 10D compared to 3.6D, for example, for the principal π-electron state

of MNA described earlier.

Extensive molecular synthesis of DVDA monomer structures has been completed with varieties of enhancing substituents yielding both centrosymmetric and noncentrosymmetric structures (Figure 14)[25]. Additionally, the theoretical calculations show that the DVDA structures are extended rigid rod structures possessing highly anisotropic polarizabilities reminiscent of mesogenic, or liquid crystal, molecular structures. Indeed, calorimetric measurements demonstrate that bis(substituted phenyl)-divinyldiacetylene monomer crystals undergo liquid crystal phase transitions above room temperature as illustrated by the DSC data for DVDA3[1,8-bis(p-propylphenyl)-octa-1,7-diene-3,5-diyne] in Figure 16. Upon heating, DVDA3 undergoes a completely reversible liquid crystal phase transition at 160°C to a stable nematic phase that is highly viscous and optically birefringent. By optical microscopy, the disinclination texture corresponds to a nematic phase. With further heating, irreversible polymerization spontaneously takes place near 180°C with exothermic heat evolved in the liquid crystal state, resulting in a highly conjugated polymer structure in a glassy, or liquid crystal, polymer state depending on the thermal annealing conditions. The resulting liquid crystal polymer is yellow-orange in color with high optical quality, insoluble in common organic solvents, and thermally stable above 210°C.

X-ray crystallographic studies[26] reveal that DVDA monomers condense at room temperature as mesogenic crystals containing linear arrays and planar sheets of DVDA sites aligned parallel with their long molecular axes. Such structural packing features are usually low temperature precursors to liquid crystal states. As an example, Figure 17 shows a typical x-ray projection of the monoclinic ($C_{2\ 1/c}$) mesogenic packing structure of DVDA3. As to the final DVDA conjugated polymer produced by liquid crystal state polymerization, the structure need not be

the same as the common linear chain polymer structure obtained from topotactic solid state polymerization of disubstituted diacetylenes of Figure 9. In fact, there is accummulating experimental evidence for the liquid crystal polymerization of DVDAs to involve some forms of extended conjugated ring structures.

Figure 18 shows typical optical transmission data for a DVDA1 polymer film contained between two glass slides. Optical transparency with low optical loss extends from the near infrared region at 2 μm to the visible red region at 0.6 μm where there is sharp onset of electronic excitations of the conjugated polymer structures. Our knowledge of three dimensionally long range ordered structures can be mapped to these liquid crystal DVDA systems (Figure 19) by maximally orienting the number N of ordered units with orienting electromagnetic fields (poling) and then locking the preferred structure in place by subsequent polymerization.

To date the new DVDA structures have exhibited several major properties:

(i) noncentrosymmetric DVDA structures exhibit large phase matched second harmonic generation;

(ii) both centrosymmetric and noncentrosymmetric DVDA monomer crystals undergo liquid crystal phase transitions;

(iii) both centrosymmetric and noncentrosymmetric DVDA monomers spontaneously react by liquid crystal state polymerization to form conjugated liquid crystal polymers displaying high optical transparency; and

(iv) by third harmonic generation measurements, unoriented centrosymmetric DVDA liquid crystal polymers exhibit unusually large third-order nonlinear optical susceptibilities $\chi^{(3)}$ that are 10^2-10^3 times larger than reference glass or quartz[27].

In summary, DVDA monomers provide crystals, liquid crystals, and glassy and liquid crystal conjugated polymer structures for studying exceptional second and third order nonlinear optical processes in organic and polymeric structures. In general, as we have summarized above, the magnitudes of the macroscopic second $\chi^{(2)}$ and third $\chi^{(3)}$ order nonlinear optical responses critically depend on the nature of the microscopic charge correlated π-electron states and also on the symmetry and degree of structural order. Such symmetry and order commonly result by virtually accidental crystal packing during single crystal growth processes. As is well known, however, liquid crystal phases possess cooperative molecular alignment that can be changed and thereby controlled by externally applied electric and magnetic fields to increase the nonlinear optical response[28]. Additionally theoretical results such as those from the SCF-CI calculations can be combined with standard guidelines and moelcular criteria that widely exist for providing liquid crystalline phases. The spontaneous formation of liquid crystalline conjugated polymer structures from orientable liquid crystal monomer phases, as exemplified by the DVDA systems, appears to provide high potential both scientifically and technologically. Having now been demonstrated for the DVDA case, there likely exist many other optically nonlinear structures possessing similar behavior and properties. Finally, the study of important nonlinear optical phenomena, processes, and device applications of organic and polymeric media comprises a new field which we refer to as Molecular Optics.

ACKNOWLEDGEMENTS

This research was supported by the Defence Advanced Research Projects Agency under Grant No. DAAK-700-77-C-0045 and the National Science Foundation Materials Research Laboratories Program under Grant No. DMR-79-23647. We gratefully thank K.N. Desai, A. Panakal, K.D. Singer, M. Kuzyk, C. Grossman, A McGhie, and P. Carroll.

FIGURE CAPTIONS

Figure 1. The molecular structure of 2-methyl-4-nitroaniline (MNA) as determined by x-ray crystallography. Key: C, carbon; N, nitrogen; O, oxygen; and H, hydrogen. Ref. 8.

Figure 2. π -electron structures.

Figure 3. Diagrammatic representation of second harmonic generation.

Figure 4. SCF-CI calculation procedure for β. Ref. 5.

Figure 5. Contour diagrams of the wave functions for the MNA ground state (bottom) and a principle excited state (top) showing charge correlations. Ref. 14.

Figure 6. The sample arrangement in the DCSHG experiment where the solution is inserted between two glass slips (a) and DC field E^{o} is applied (b). Ref. 12.

Figure 7. Frequency dependence of β_x for MNA. Key: +, experimental β_x^{exp} data points; and -, theoretical β_x^{d} curve accounting for solvent shift effect. Ref. 12.

Figure 8. Optical absorption spectra of MNA dissolved in dioxane (solid line) and in gas phase (dashed line) showing solvent shift. Ref. 12.

Figure 9. Solid state polymerization of disubstituted diacetylene monomers to form crystalline polymer chains.

Figure 10. Monoclinic unit cell of the diacetylene polymer of 1,6-bis(2,4-dinitrophenoxy)-2,4-hexadiyne (DNP). Ref. 21.

Figure 11. Comparison of MNA (a) and MNADA (b) β_x values as measured by DCSHG. Ref. 22.

Figure 12. The second harmonic $I^{2\omega}$ of NTDA microcrystals relative to the second harmonic intensity of lithium iodate ($LiIIO_3$) powder $I^{2\omega}$ with increasing x-ray induced polymerization. Ref. 22.

Figure 13. Classes of disubstituted diacetylene structures exhibiting phase matched second harmonic generation.

Figure 14. Bis(phenyl)-divinyldiacetylene monomers with various substituent groups.

Figure 15. Contour diagrams of the wavefunction for the DVDA1 ground state (bottom) and the principle singlet (^1B_u) excited state (top) showing delocalization and charge correlations. Ref. 24.

Figure 16. DSC calorimetric thermogram of DVDA3 showing liquid crystal phase transition followed by liquid crystal polymerization. Ref. 25.

Figure 17. Mesogenic crystal structure of DVDA3 showing linear arrays and planar sheets as possible precursors to liquid crystal state. Ref. 26.

Figure 18. Optical transmission of DVDA1 polymer film over the near infrared-visible range. Ref. 27.

Figure 19. Experimental poling configuration for orienting DVDA monomers and polymers in an applied electromagnetic field while monitoring the nonlinear optical signal ω_3 derived from the inputs ω_1 and ω_2. Ref. 27.

REFERENCES

1. R.W. Hellwarth, J. Opt. Soc. Amer. 67, 1 (1977).

2. H.M. Gibbs, S.L. McCall and T.N.C. Venkatesan, Phys. Rev. Lett. 36, 1135 (1976).

3. See, for example, A.F. Garito and K.D. Singer, Laser Focus 18, 59 (1982).

4. C. Sauteret, J.P. Hermann, R. Frey, F. Padere, J. Ducuing, R. Baughman, and R. Chance, Phys. Rev. Lett. 36, 956 (1976).

5. S.J. Lalama and A.F. Garito, Phys. Rev. A20, 1179 (1979).

6. C. Flytzanis in Nonlinear Optical Properties of Organic and Polymer Materials, D. Williams, ed., ACS Symp. Ser. No. 233 (1983).

7. B.F. Levine, C.G. Bethea, C.D. Thurmond, R.T. Lynch, and J.L. Bernstein, J. Appl. Phys. 50, 2523 (1979).

8. G.F. Lipscomb, A.F. Garito and R.S. Narang, J. Chem. Phys. 75, 1509 (1981).

9. Nonlinear Optical Properties of Organic and Polymer Materials, D. Williams, ed., ACS Symp. Ser. No. 233 (1983).

10. N. Bloembergen, Nonlinear Optics (W.A. Benjamin Inc., New York, 1965).

11. C.C. Teng and A.F. Garito, Phys. Rev. Lett. 50, 350 (1983).

12. C.C. Teng and A.F. Garito, Phys. Rev. B28, 6766 (1983).

13. O. Zammani'Khamiri and A.F. Garito, to be published.

14. O. Zammani'Khamiri, C.C. Teng and A.F.

Garito, to be published.

15. S.J. Lalama, K.D. Singer, A.F. Garito and K.N. D-sai, Appl. Phys. Lett. 39, 940 (1981).

16. K.D. Singer and A.F. Garito, J. Chem. Phys. 75, 3572 (1981).

17. See, for example, A.T. Amos and B.L. Burrows, Adv. Quantum Chem. 7, 289 (1973) and references therein.

18. A.F. Garito, K.D. Singer, K. Hayes, G.F. Lipscomb, S.J. Lalama, and K.N. Desai, J. Opt. Soc. Amer. 70, 1399 (1980).

19. See, for example, G. Wegner in Molecular Metals, W. Hatfield, ed., Plenum (1979) and references therein.

20. J.E. Sohn, A.F. Garito, K.N. Desai, R.S. Narang and M. Kuzyk, Makromol. Chem. 180, 2975 (1979).

21. A.R. McGhie, G.F. Lipscomb, A.F. Garito, K.N. Desai, and P. Kalyanaraman, Makromol. Chem. 182, 965 (1981).

22. K.D. Singer and A.F. Garito, to be published.

23. A.F. Garito, K.D. Singer and C.C. Teng, in Ref. 9.

24. O. Zammani'Khamiri and A.F. Garito, to be published.

25. A. Panakal, K.N. Desai, A.R. McGhie and A.F. Garito, to be published.

26. K.Y. Wong,, K.N. Desai, P. Carroll and A.F. Garito, to be published.

27. K.Y. Wong, C.C. Teng and A.F. Garito, J. Opt. Soc. Amer, in press.

28. See, for example, G. Meredith, J.G. Van Dusen and D.J. Williams, in ref. 9 and references therein.

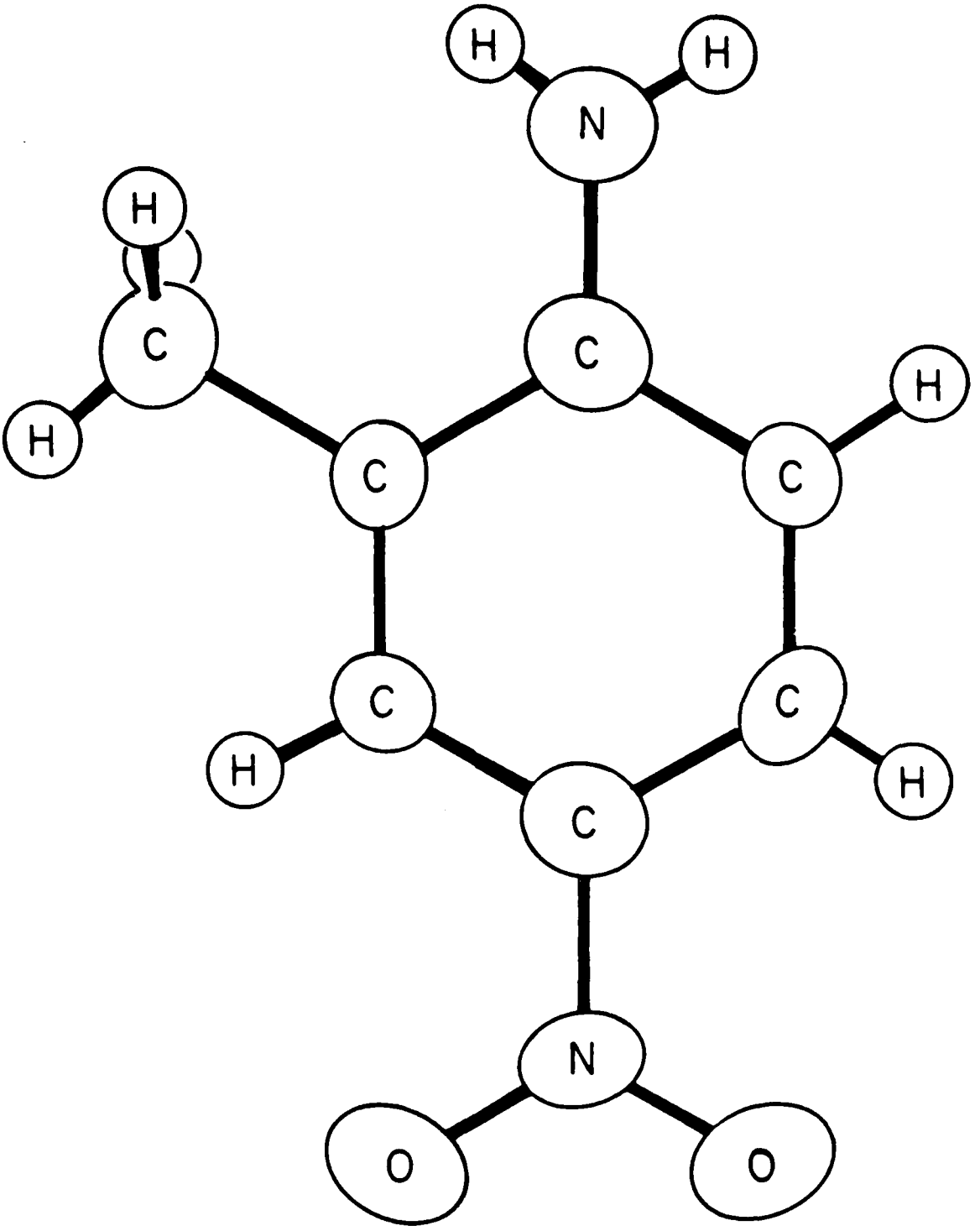

MNA (2-METHYL-4-NITROANILINE)

Fig. 1

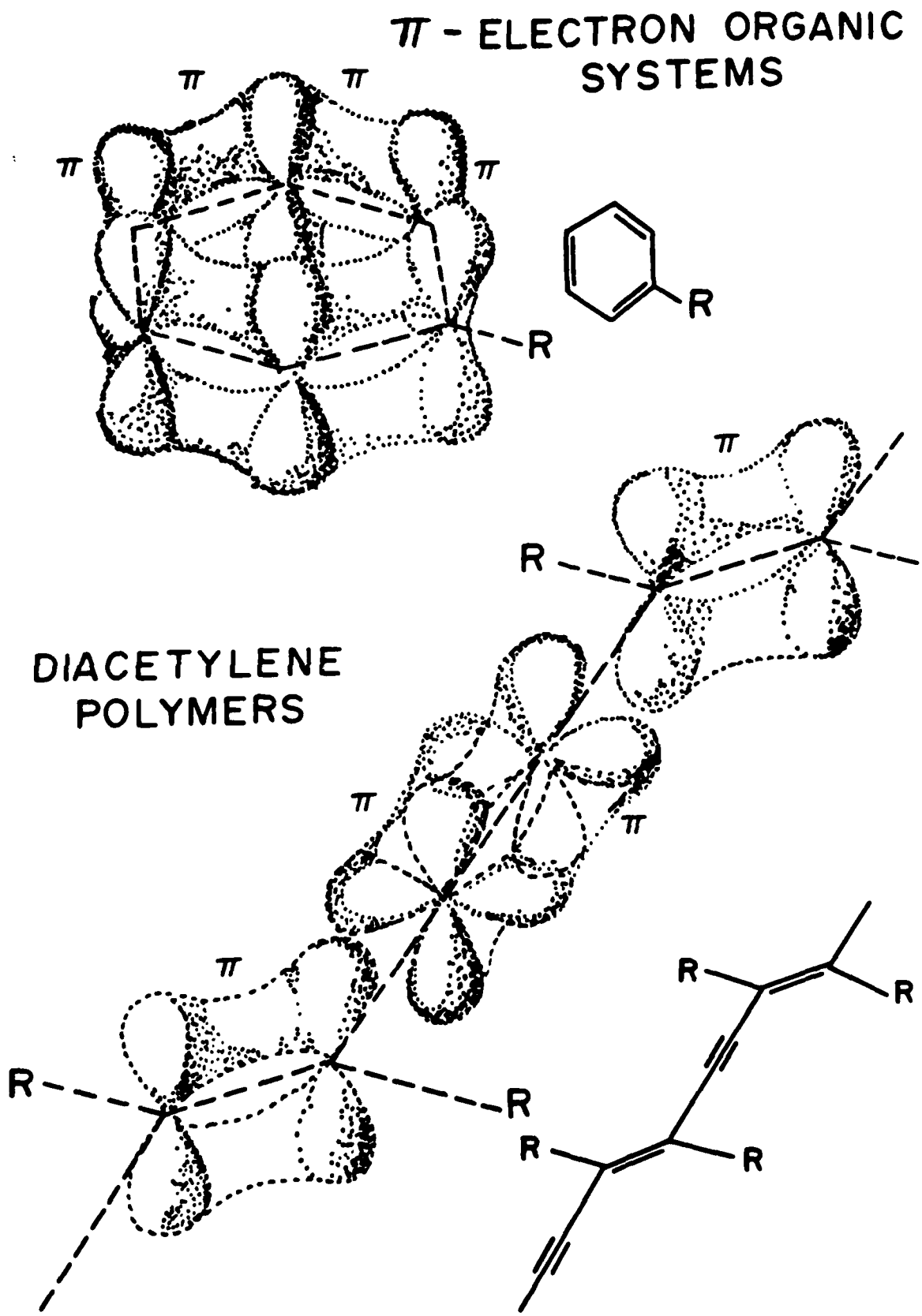
π - ELECTRON ORGANIC SYSTEMS
π
π
π
π
R
R
π
R
DIACETYLENE POLYMERS
π
π
π
R
R
R
R
R
R

Fig. 2

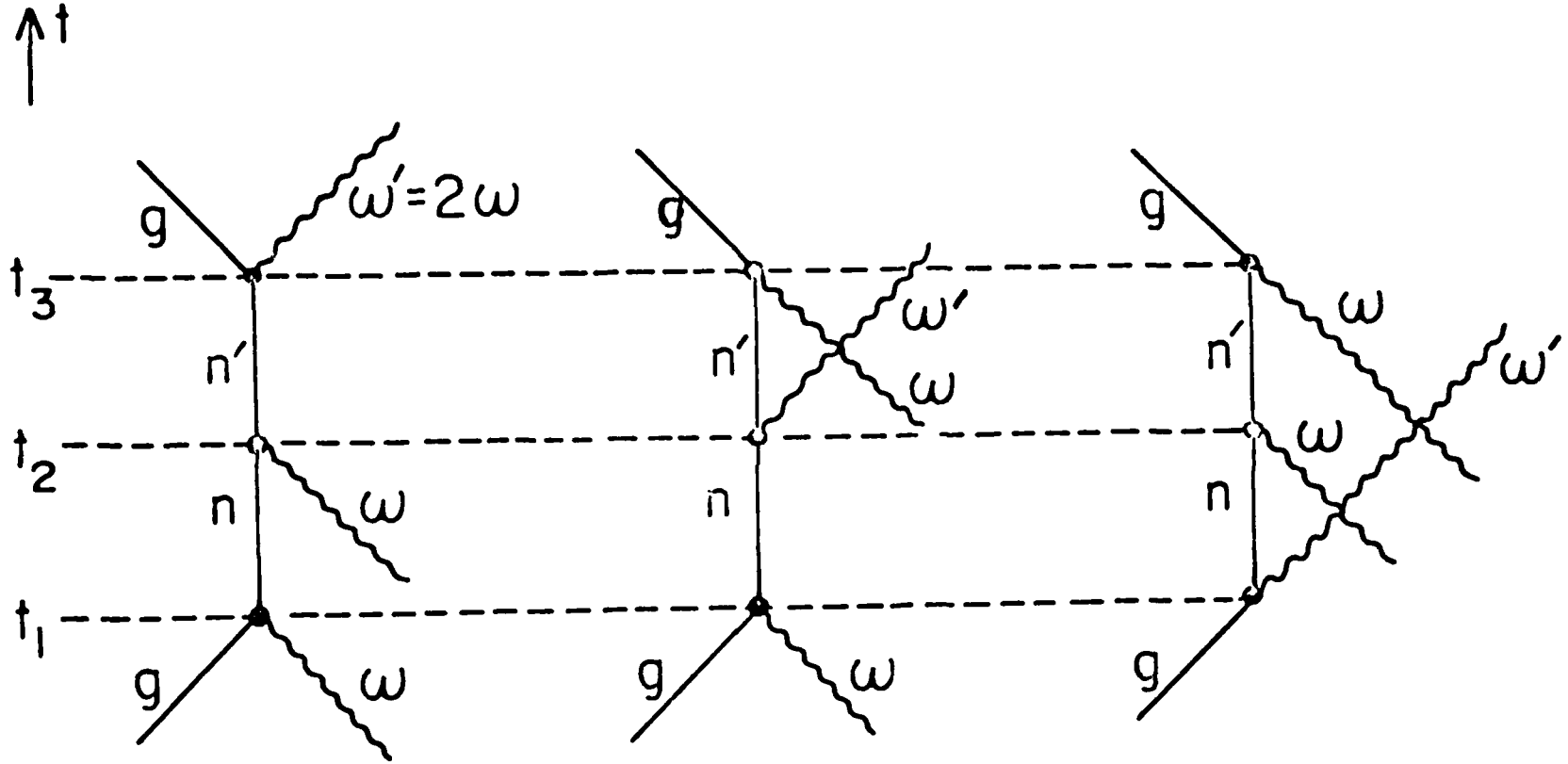

Fig. 3

ELECTRONIC POLARIZATION

$$P_i^{2\omega} = \sum_{j,k} \beta_{ijk}(-2\omega;\omega,\omega)\, e_j^{\omega}\, e_k^{\omega}$$

SCF – CI CALCULATION PROCEDURE FOR MOLECULAR SECOND ORDER OPTICAL SUSCEPTIBILITIES.

I. GROUND STATE CALCULATION TO DETERMINE ONE-ELECTRON LEVEL.

- MOLECULAR HARTREE-FOCK CALCULATION
- EXPERIMENTAL PHOTOEMISSION DATA USED FOR VERIFICATION OF 1-ELECTRON LEVEL.

II CALCULATION OF MANY-BODY EXCITED STATE ENERGIES AND TRANSITION MOMENTS

- CONFIGURATION INTERACTION CALCULATION FOR EXCITED STATES
- ULTRAVIOLET ABSORPTION DATA USED FOR VERIFICATION OF EXCITED STATES

III. CALCULATION OF MOLECULAR SECOND ORDER SUSCEPTIBILITY

- SUSCEPTIBILITY DETERMINED DIRECTY FROM SECOND-ORDER PERTURBATION THEORY
- COMPARISON OF CALCULATION WITH RESULTS OF D.C. INDUCED SECOND HARMONIC GENERATION

Fig. 4

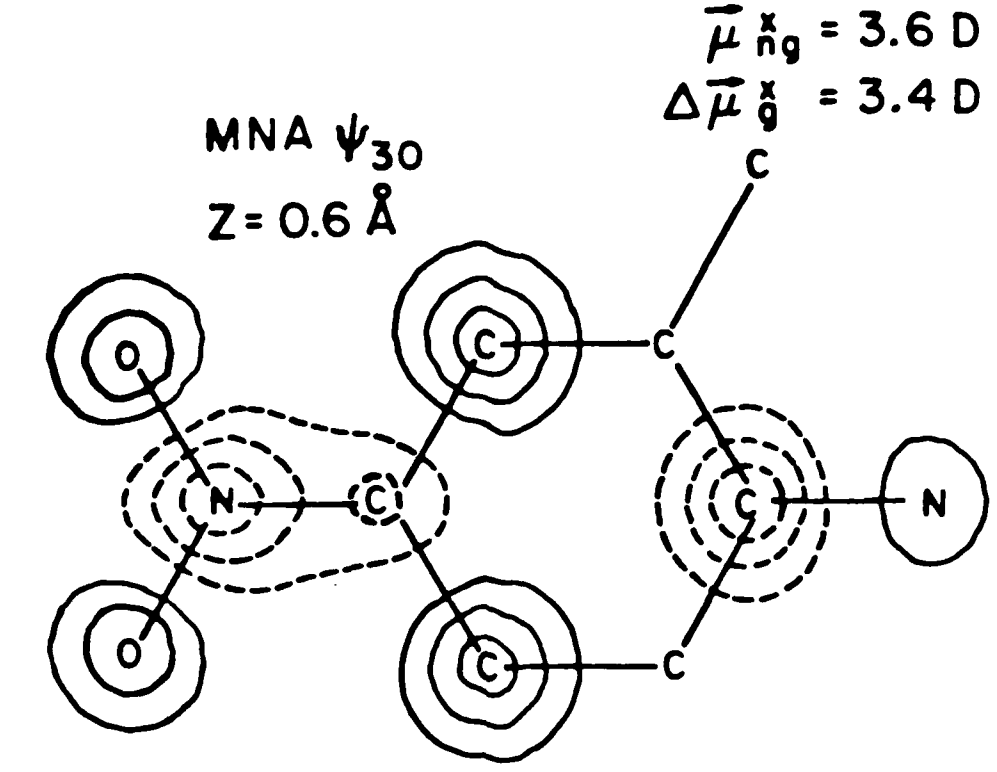
$\vec{\mu}^{x}_{ng} = 3.6$ D
$\Delta\vec{\mu}^{x}_{g} = 3.4$ D
MNA ψ_{30}
Z = 0.6 Å
O
O
N
C
C
C
C
C
C
C
N
EXCITED STATE

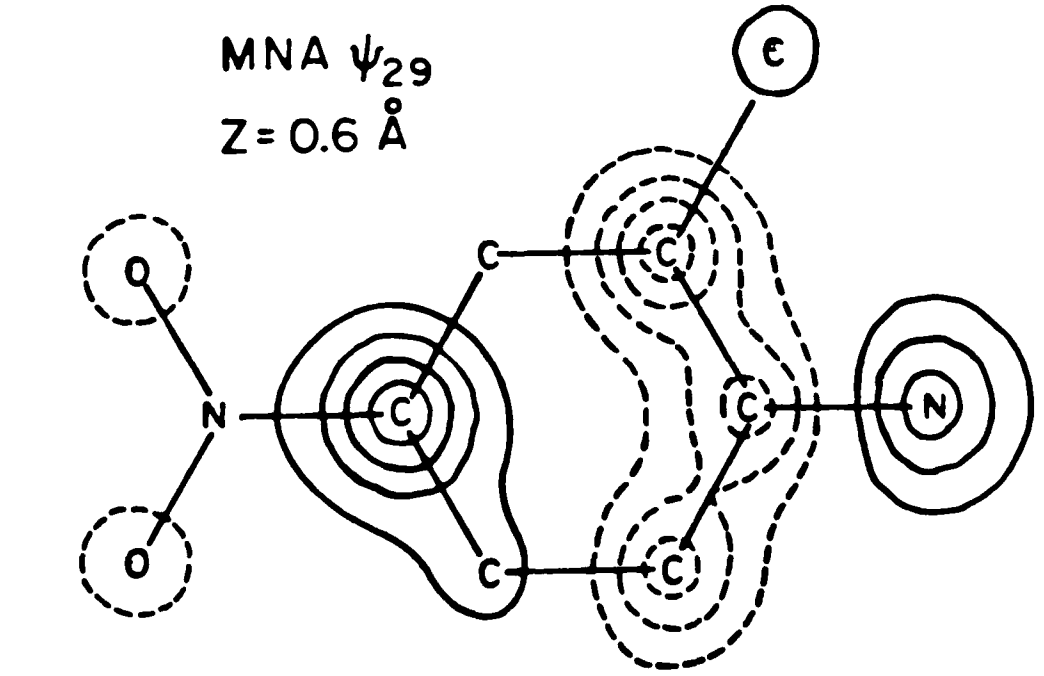
MNA ψ_{29}
Z = 0.6 Å
O
O
N
C
C
C
C
C
C
C
N
GROUND STATE

Fig. 5

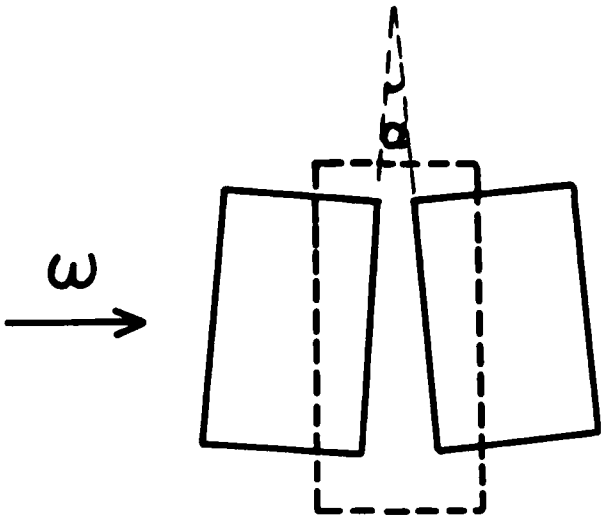

(a)

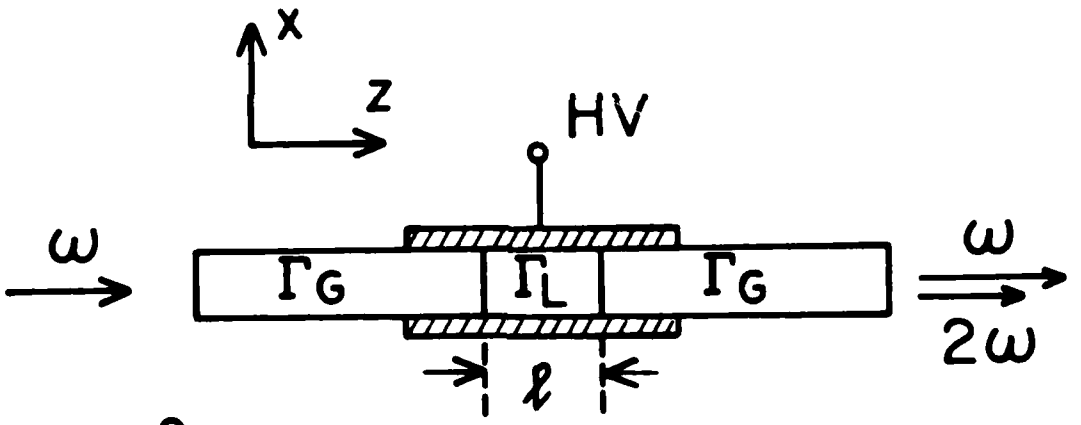

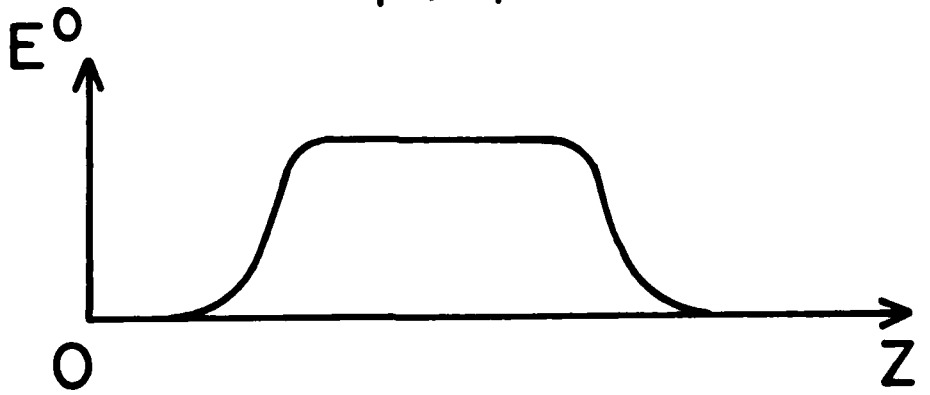

(b)

Fig. 6

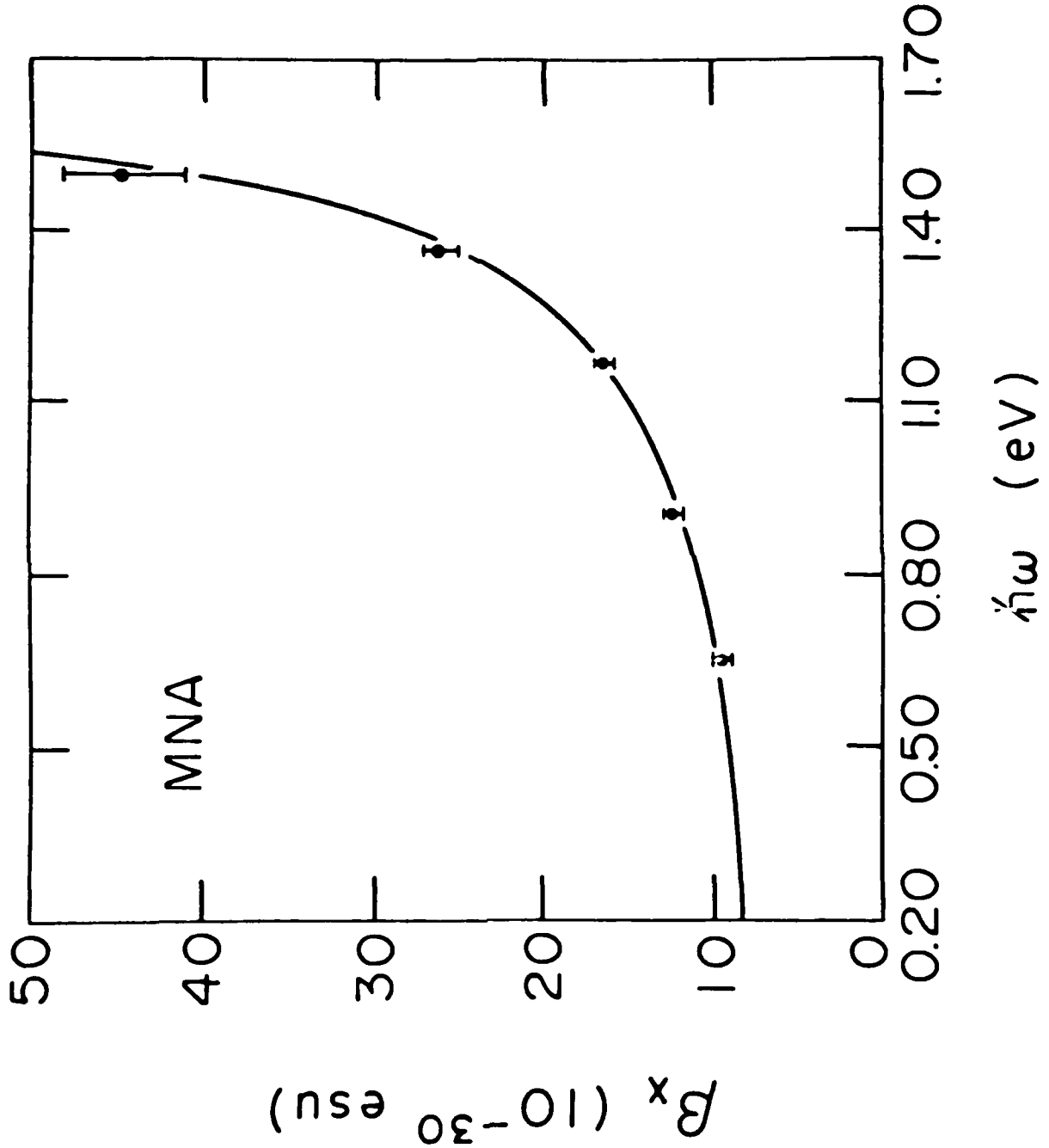
MNA
β_x (10^{-30} esu)
$\hbar\omega$ (eV)
0
10
20
30
40
50
0.20
0.50
0.80
1.10
1.40
1.70

Fig. 7

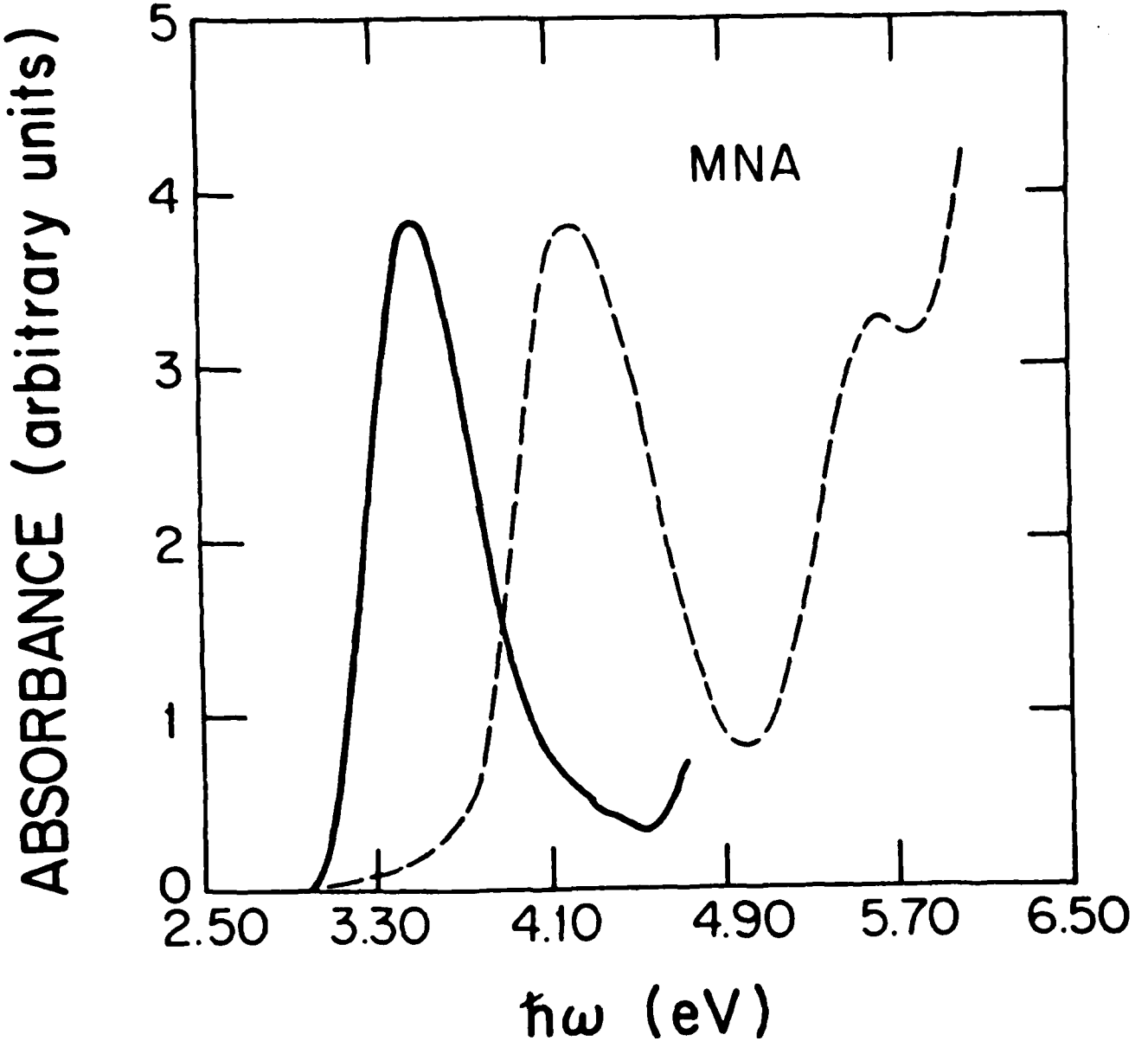
ABSORBANCE (arbitrary units)
0
1
2
3
4
5
MNA
2.50
3.30
4.10
4.90
5.70
6.50
ħω (eV)

Fig. 8

SOLID STATE POLYMERIZATION

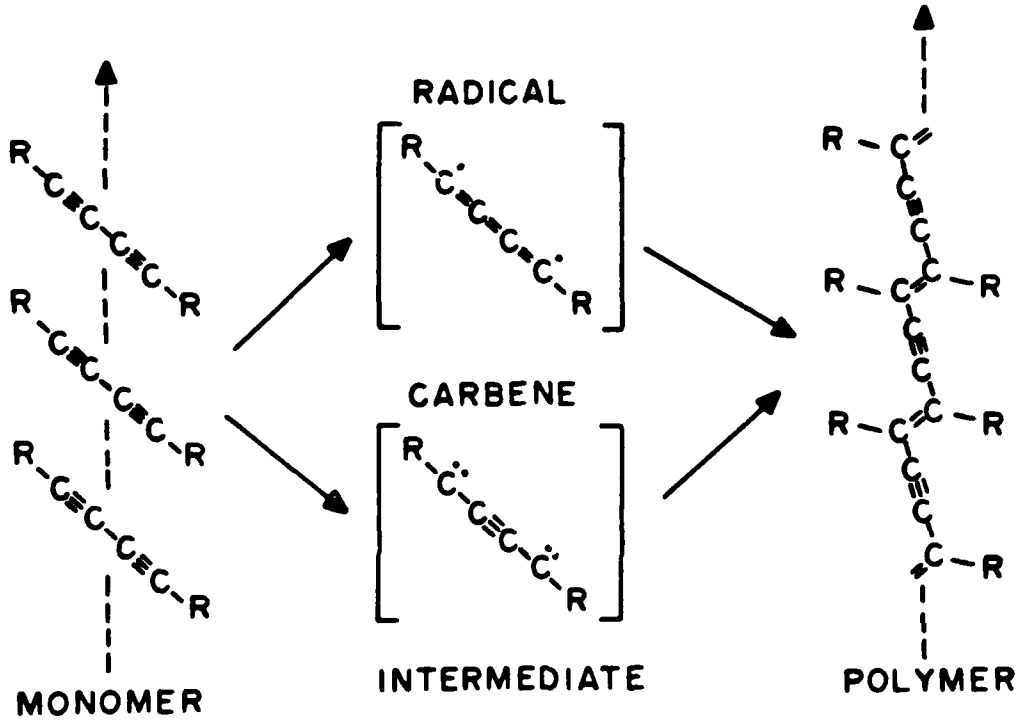

INITIATION :

- THERMAL { $\Delta H = -32$ kcal/mole, $E_A = 25\text{-}30$ kcal/mole
- PHOTO — q. eff. = 10-100
- X-RAY } q. eff. = 1×10^{12}, $E = 1\ \mu J/cm^2$
- E-BEAM }
- MECHANICAL

PROPERTIES :

- 3D LRO
- SEMICONDUCTOR $E_G > 2$ eV
- OPTICAL BIREFRINGENCE
- EXCEPTIONAL RADIATION DAMAGE RESISTANCE
- HIGH STRENGTH

Fig. 9

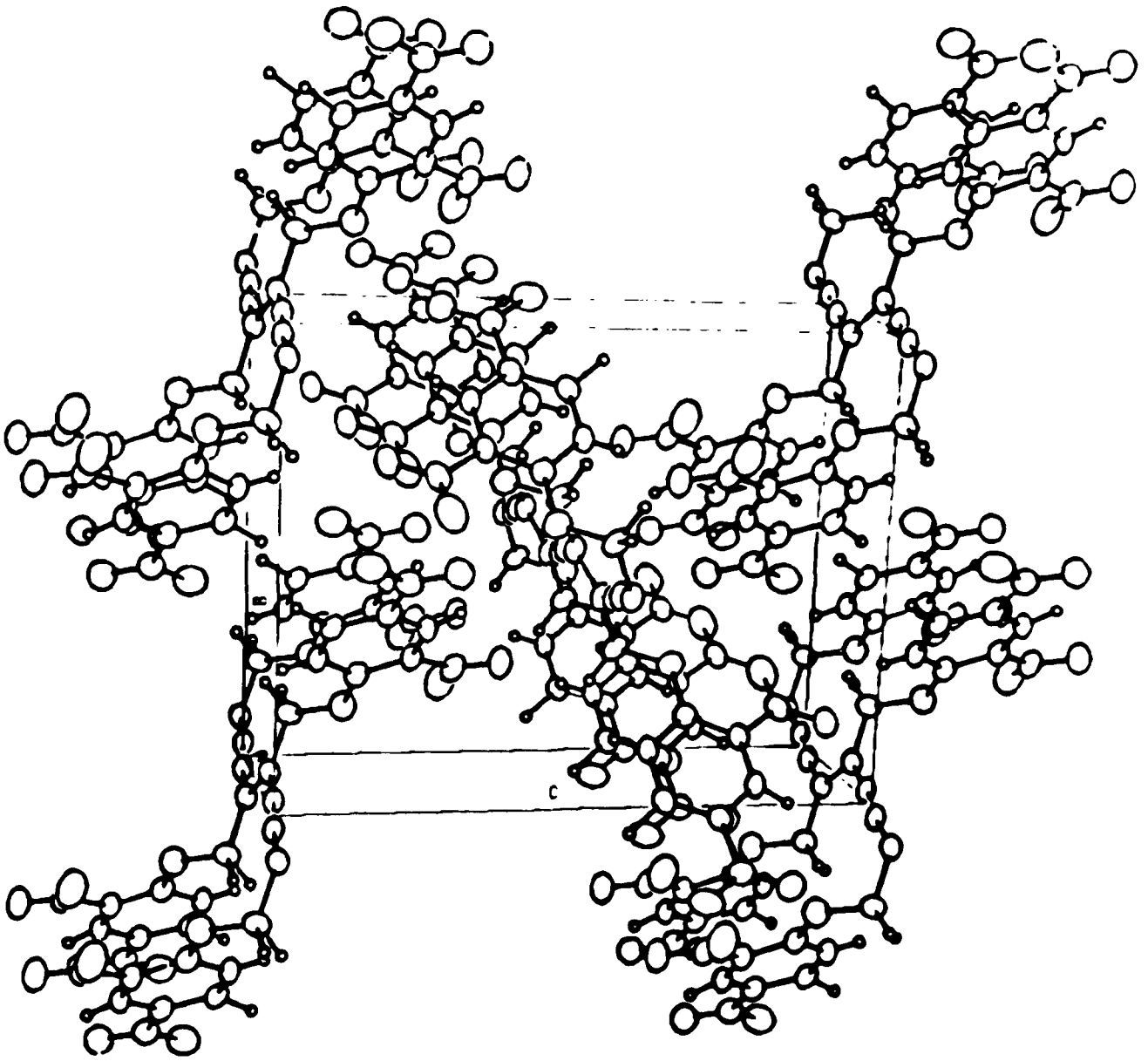

Fig. 10

(a)

MNA

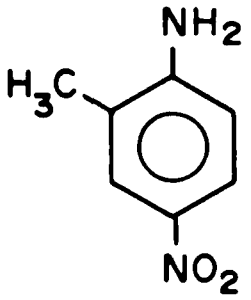

$\beta_x = 17 \pm 1 \times 10^{-30}$ esu (1.06 μm)

(b)

MNADA

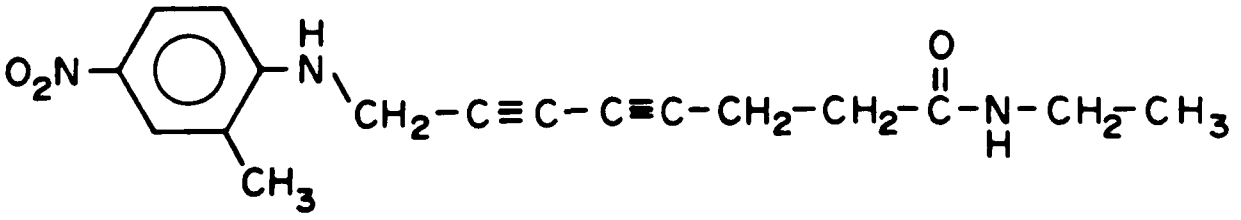

$\beta_x = 17 \pm 1 \times 10^{-30}$ esu (1.06 μm)

Fig. 11

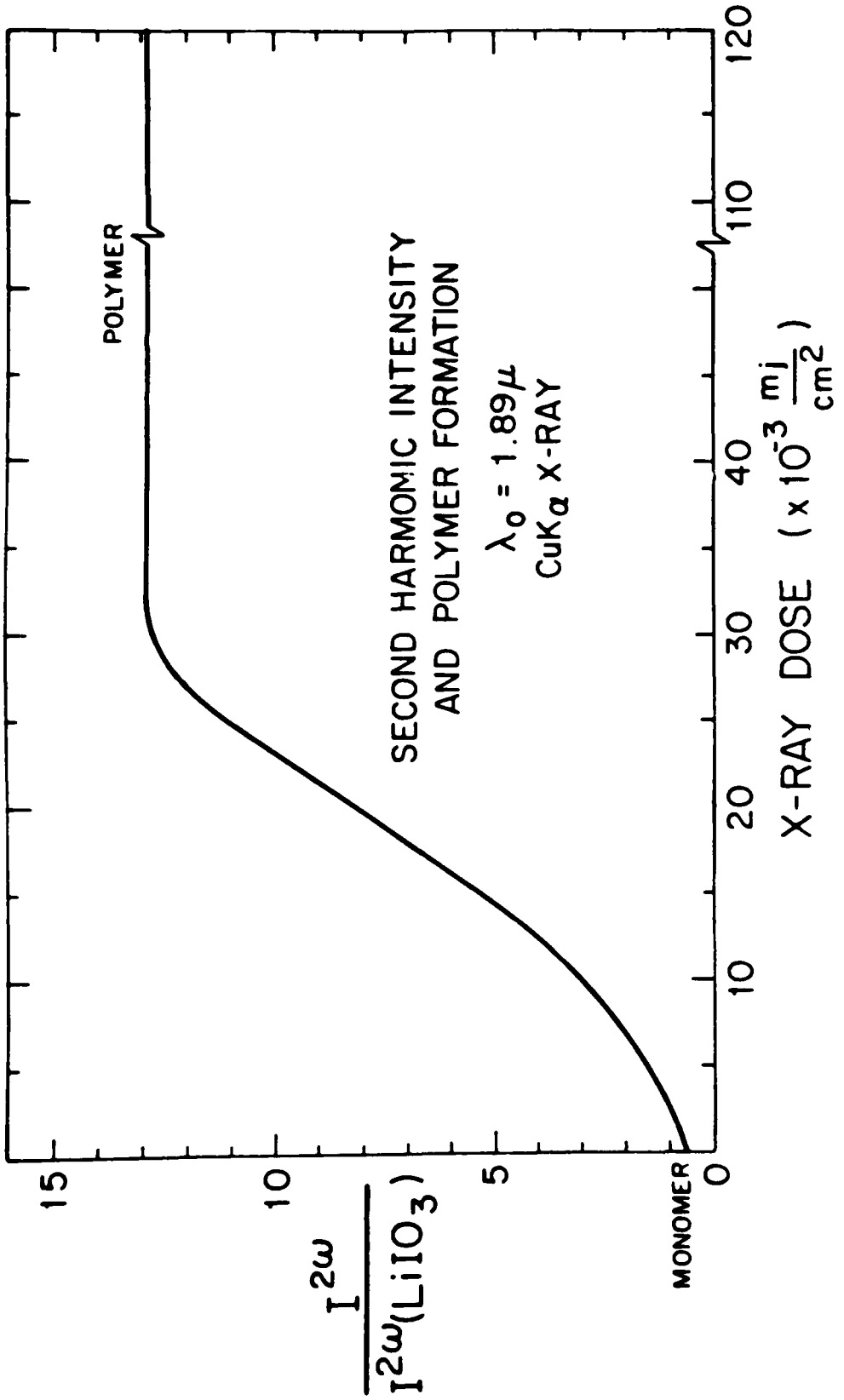
SECOND HARMONIC INTENSITY
AND POLYMER FORMATION
$\lambda_o = 1.89\mu$
CuK_α X-RAY
POLYMER
MONOMER
$\frac{I^{2\omega}}{I^{2\omega}(LiIO_3)}$
X-RAY DOSE ($\times 10^{-3}$ $\frac{mj}{cm^2}$)
0
5
10
15
20
30
40
110
120

Fig. 12

DIACETYLENE POLYMERS: PHASE MATCHED SECOND HARMONIC GENERATION

$$R-(CH_2)_n-C\equiv C-C\equiv C-(CH_2)_m-R'$$

R PENDANT SIDE GROUP

- NITROANILINES

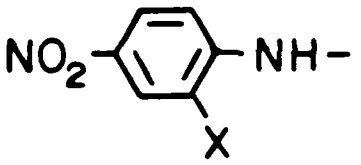

X = H, CH_3, CF_3, NO_2

- QUINOIDS

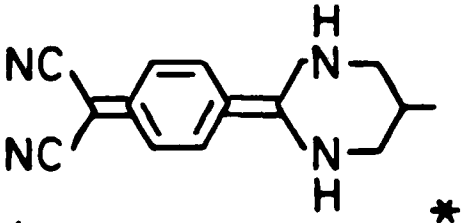

R' = CH_3, AMIDES*

n = 1, 2 ; m = 2 - 11

Fig. 13

DIVINYLDIACETYLENES

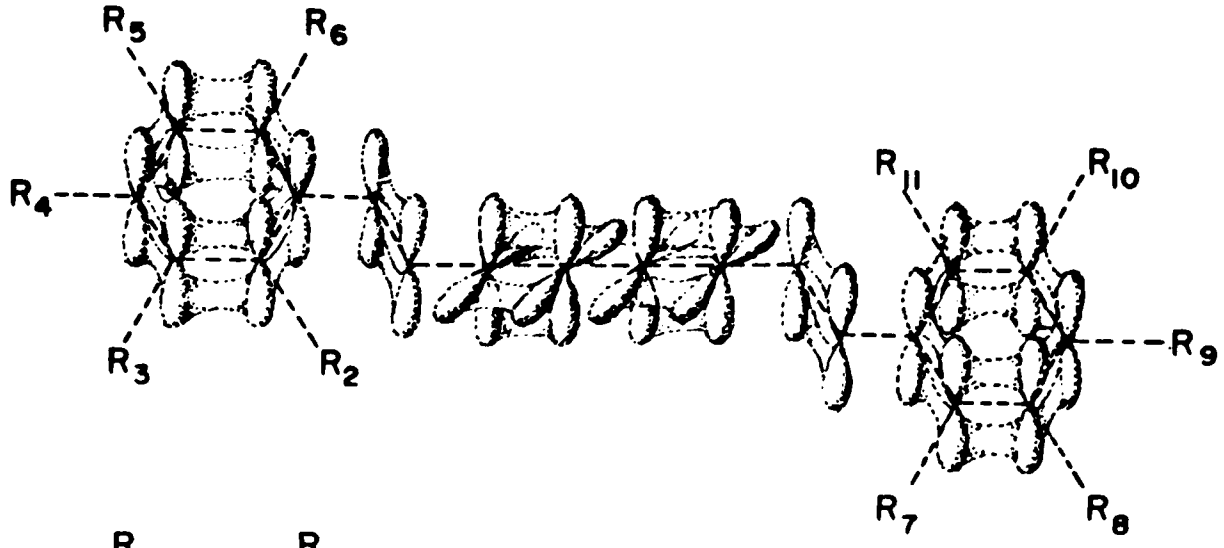

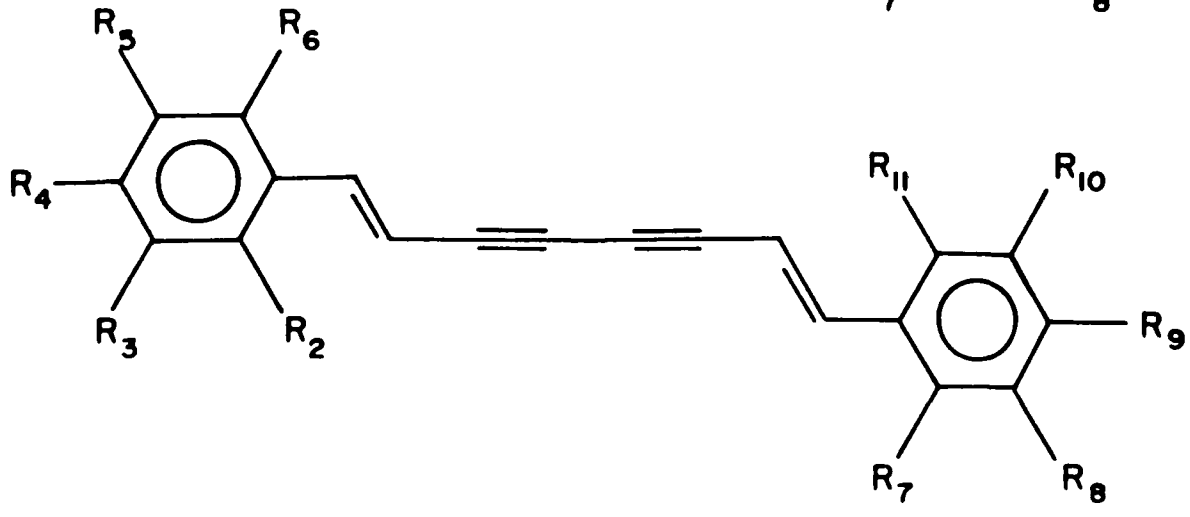

$R_1 - R_{11}$: H , $(CH_2)_{n-1}-CH_3$, $(C_6H_4)_n$-H, Cl , CN , NO_2 , CF_3

Fig. 14

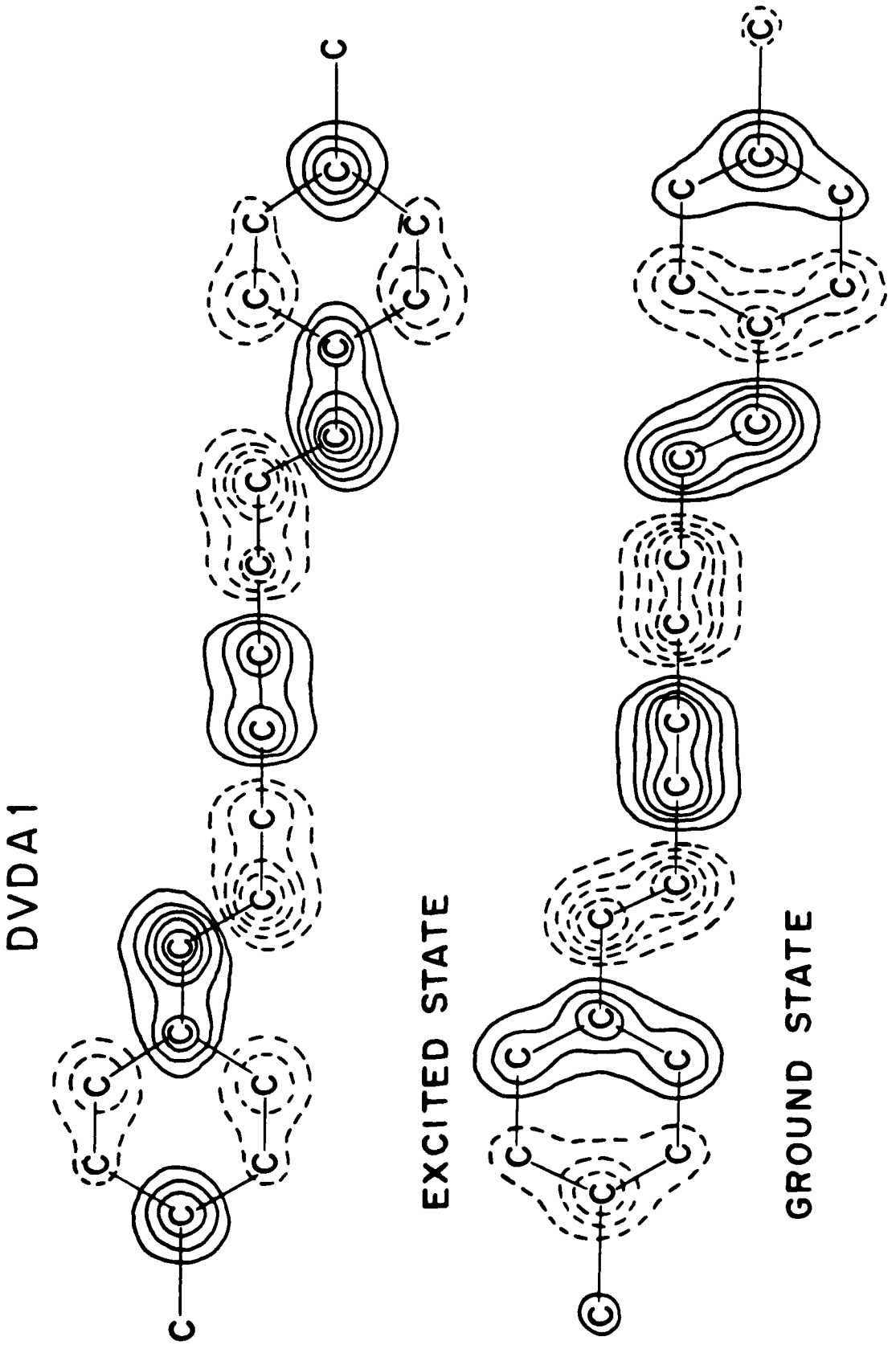

Fig. 15

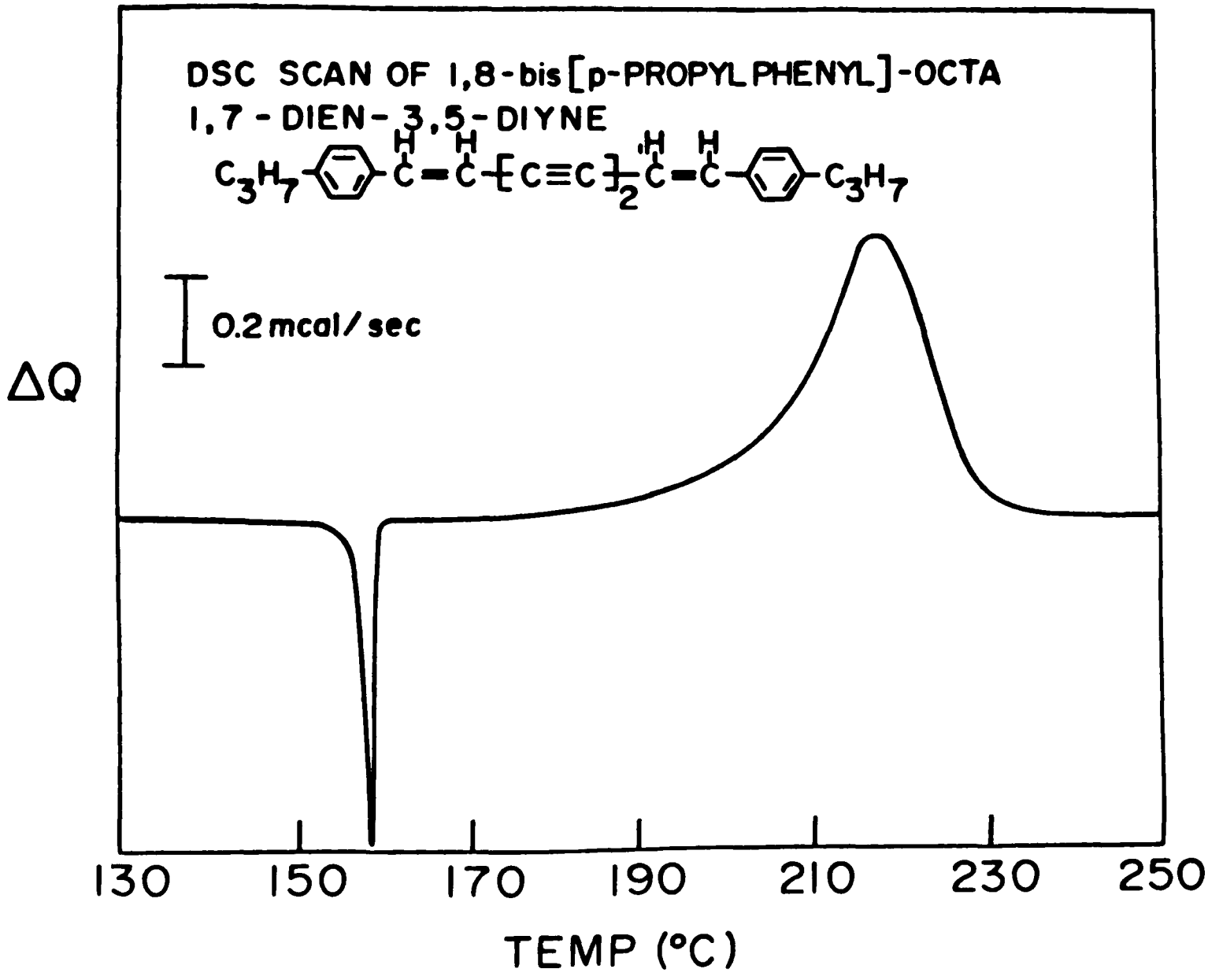
DSC SCAN OF 1,8-bis[p-PROPYLPHENYL]-OCTA
1,7-DIEN-3,5-DIYNE
C_3H_7
C_3H_7
0.2 mcal/sec
ΔQ
130
150
170
190
210
230
250
TEMP (°C)

Fig. 16

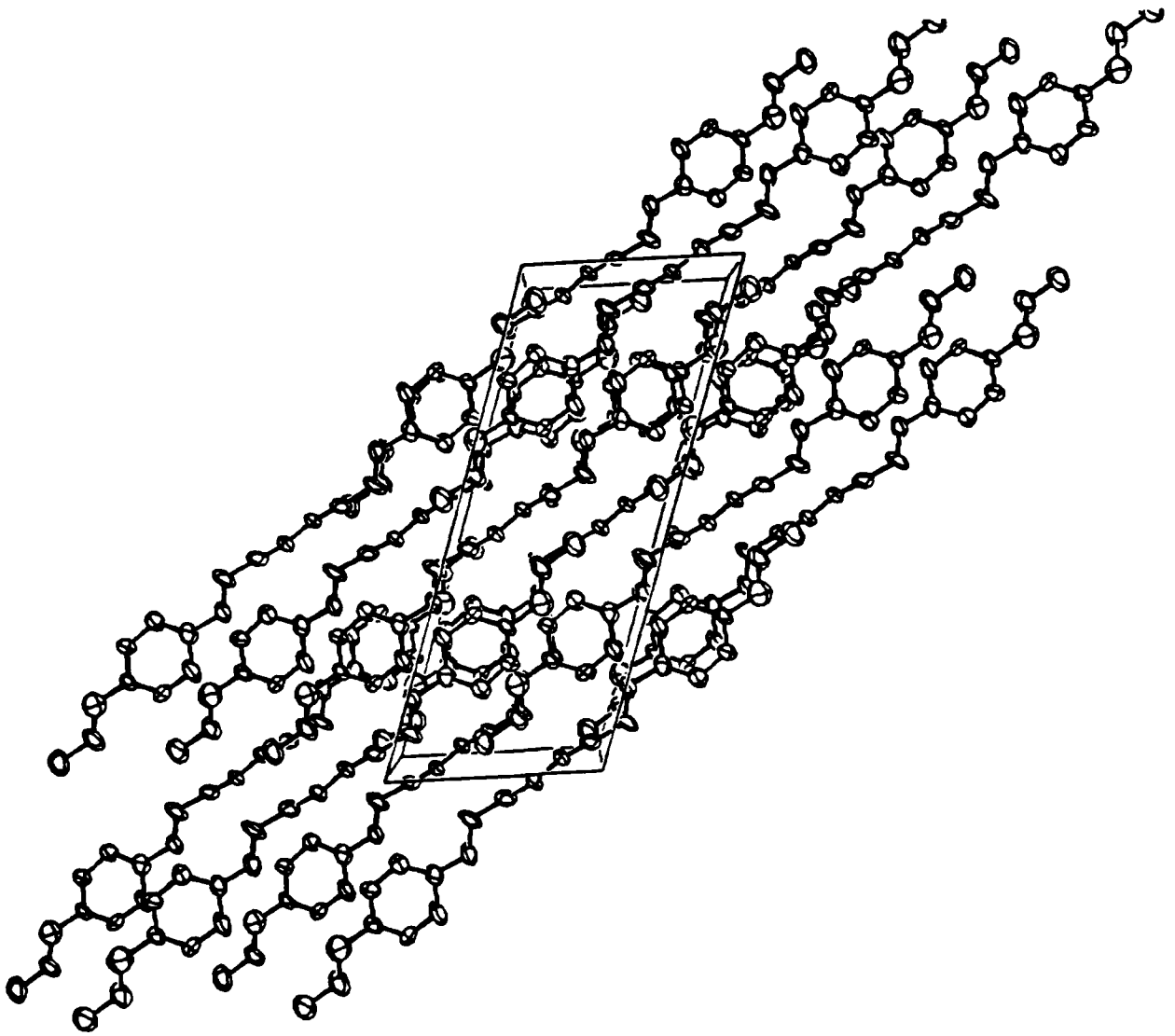

Fig. 17

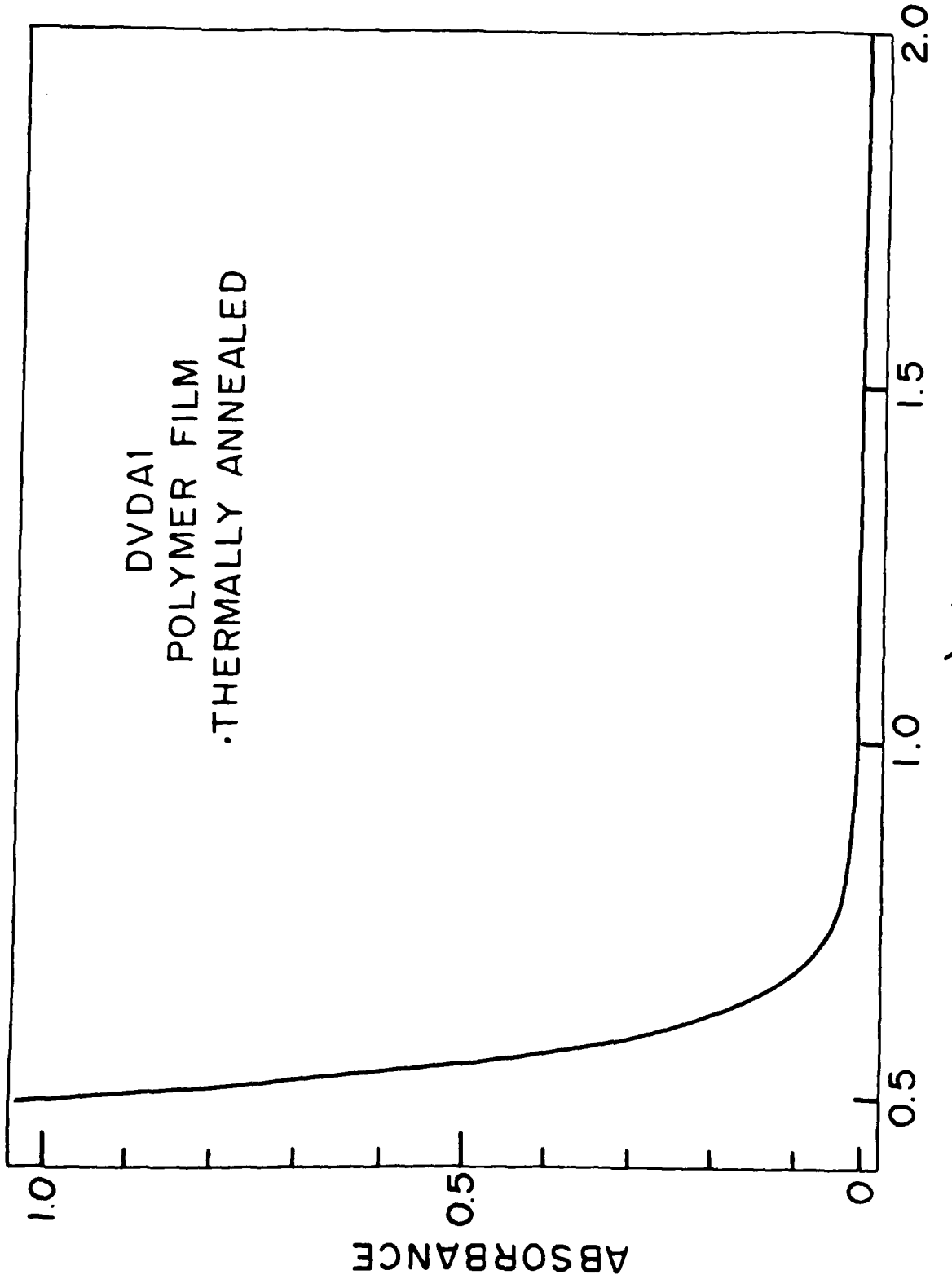
DVDA1
POLYMER FILM
·THERMALLY ANNEALED
ABSORBANCE
1.0
0.5
0
0.5
1.0
1.5
2.0
λ (μ)

Fig. 18

ORIENTATION OF DVDA BY APPLIED EM FIELDS

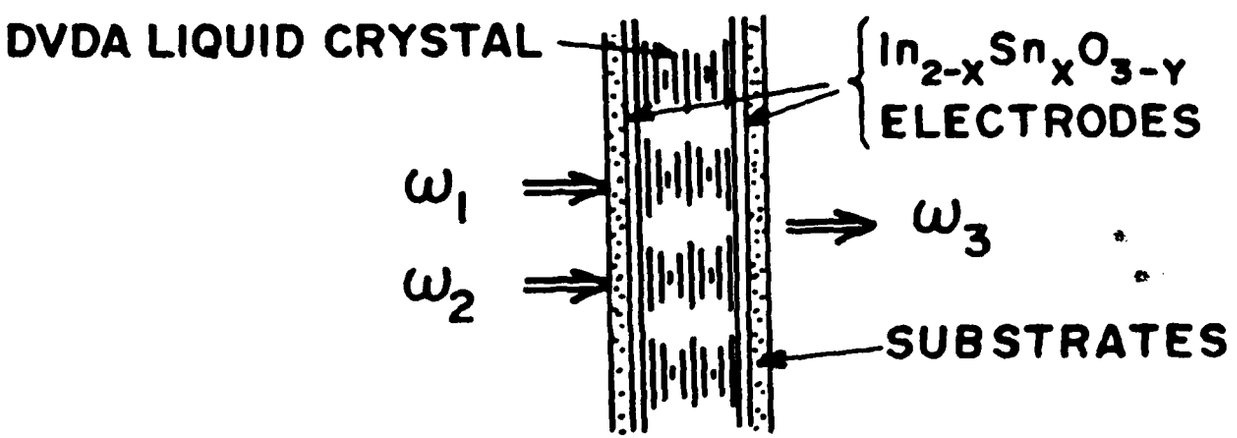

$$\chi^{(2)}(-\omega_3;\omega_1,\omega_2) = \langle N\rangle f^{\omega_1} f^{\omega_2} f^{\omega_3} \langle \beta_{ijk}(-\omega_3;\omega_2,\omega_1)\rangle$$

$\langle N\rangle$ NUMBER OF ORIENTED UNITS

- LOCK IN BY POLYMERIZATION

Fig. 19

END

DTIC

5-86